Fractures in regions of adaptive modeling and remodeling of central tarsal bones in racing Greyhounds

Mary Sarah Bergh, DVM, MS; Alessandro Piras, Dr Med Vet; Valerie F. Samii, DVM; Steven E. Weisbrode, VMD, PhD; Kenneth A. Johnson, MVSc, PhD

Objective—To evaluate and compare bone modeling and remodeling in fractured and nonfractured central tarsal bones (CTBs) of racing Greyhounds.

Sample—Paired cadaveric tarsi from 6 euthanized racing Greyhounds with right CTB fractures and 6 racing Greyhounds with other nontarsal injuries.

Procedures—CTBs were dissected and fractured CTBs were reconstructed. Central tarsal bones were evaluated through standard and nonscreen high-detail radiography, computed tomography, and histologic examination. The bone mineral density (BMD) was calculated adjacent to fracture planes and as a gradient on sagittal computed tomographic images. Sagittal and transverse plane sections of bone were obtained and submitted for subjective histologic assessment. Linear mixed-effects models were used to compare findings.

Results—Fractured right CTBs had greater BMD in the dorsal and midbody regions of the sagittal plane sections than did nonfractured CTBs. The BMD ratios from bone adjacent to the dorsal slab fracture planes were not different between fractured and nonfractured right CTBs.

Conclusions and Clinical Relevance—Findings supported the existence of site-specific bone adaptation in CTBs of Greyhounds, with modeling and remodeling patterns that were unique to fractured right CTBs. The dorsal and midbody regions of fractured bones had greater BMD, and fractures occurred through these zones of increased BMD. (*Am J Vet Res* 2012;73:375–380)

Fracture of cuboidal bones in the foot is common in human and other mammalian athletes. Fatigue fracture of these bones, particularly of the central (navicular) tarsal bone, is believed to be caused by repetitive loading, site-specific bone modeling and remodeling, and subsequent fatigue failure.[1–3] Racing Greyhounds are excellent subjects by which to study adaptive modeling and fatigue because their right and left limbs are asymmetrically loaded during training and racing counterclockwise on oval tracks. Located on the medial aspect of the outside limb, right CTBs are subjected to substantially greater compressive loads than are left CTBs and consequently sustain as much as 96% of fractures.[4] An increase in load on the right CTB causes that bone to increase in size and sustain a greater amount of matrix microdamage than the contralateral bone.[1,2]

Catastrophic failure of the CTB has been proposed to be due to coalescence of the microcracks, inadequate reparative response, or weakness during bone resorption amid an extensive remodeling process within the bone.[1,5–7] However, fractured CTBs from racing Greyhounds have not been rigorously evaluated and the nature of any important differences between fractured and nonfractured right CTBs remains unclear.

Abbreviations

BMD	Bone mineral density
CT	Computed tomography
CTB	Central tarsal bone
PMMA	Polymethylmethacrylate
PPED	Dipotassium phosphate equivalent density
ROI	Region of interest

Received October 4, 2010.
Accepted February 15, 2011.
From the Departments of Veterinary Clinical Sciences and Veterinary Biosciences, College of Veterinary Medicine, The Ohio State University, Columbus, OH, 43210 (Bergh, Samii, Weisbrode, Johnson); and Oakland Referrals, 55°/b Bridge St, Banbridge, BT323JL, Northern Ireland (Piras). Dr. Bergh's present address is Department of Veterinary Clinical Sciences, College of Veterinary Medicine, Iowa State University, Ames, IA 50011. Dr. Johnson's present address is Faculty of Veterinary Science, University of Sydney, Sydney, NSW 2006, Australia.
This manuscript represents a portion of a thesis submitted by Dr. Bergh to The Ohio State University as partial fulfillment of the requirements for a Master of Science degree.
Supported by a grant to Dr. Johnson from the AO Research Foundation.
Presented in abstract form at the American College of Veterinary Surgeons Veterinary Symposium, San Diego, October 2008.
The authors thank Amy Lehman for statistical consultation and Nancy Weber, Melissa Sama, and Dr. Katy Townsend for technical assistance.
Address correspondence to Dr. Bergh (msbergh@iastate.edu).

The purpose of the study reported here was to evaluate CTBs from skeletally mature racing Greyhounds and determine whether there were site-specific modeling and remodeling responses in naturally occurring fractures in right CTBs, with use of standard and contact radiography, CT, and histologic evaluation. We hypothesized that unique site-specific modeling and remodeling patterns would be detected in fractured bones. Specifically, we hypothesized that the BMD of fractured right CTBs would be greater than that of intact right and left CTBs and that dorsal slab fractures would occur through a transition zone between bone tissues of differing densities.

Materials and Methods

Animals—Pelvic limbs were collected from 12 skeletally mature racing Greyhounds after euthanasia. Dogs were euthanized at their owners' request after CTB fracture or other nontarsal racing injuries. Reasons for euthanasia were unrelated to the study. Dogs were excluded when there was gross or radiographic evidence of a reparative response associated with the tarsal fractures. The harvested pelvic limbs were stored at –80°C until used in the study. Details about the age, sex, weight, and racing history of the dogs were not available.

Radiographic evaluation of the tarsus—Mediolateral, plantarodorsal, plantarolateral-dorsomedial oblique, and plantaromedial-dorsolateral oblique radiographic views of each tarsus were obtained to determine injury status. The radiographs were evaluated for evidence of tarsal bone fractures. Central tarsal bone fractures were classified into 5 types in accordance with a preexisting scheme.[8]

CT evaluation of the tarsus—Measurement of BMD was performed by use of a fourth-generation helical CT scanner[a] and a high-detail bone algorithm (**Figure 1**). Limbs were positioned in the scanner with foam blocks and tape. A series of 1-mm contiguous transverse and sagittal plane images was acquired by use of a 512 × 512 matrix (voxel element, 0.075 mm^3) and a 140-mm field of view. A dipotassium phosphate phantom[b] was included with each specimen. The phantom contained 5 cylinders of known tissue-equivalent densities; these included dipotassium phosphate solution (200, 100, and 50 mg/mL), water, and high-density polyethylene. Use of the phantom enabled internal calibration and direct quantification of BMDs. Computed tomographic attenuation data were converted from Hounsfield units to PPED (mg/mL) to enable comparisons with data obtained from other scanners by use of a regression equation as described elsewhere.[9] The CT images were evaluated for tarsal fractures, and the configurations of the CTB fractures were recorded.

CTB reconstruction and imaging—Central tarsal bones were dissected from each tarsus. Fractured CTBs were anatomically reconstructed with the aid of cyanoacrylate.[c] All CTBs were fixed in neutral-buffered 10% formalin and embedded in PMMA under vacuum.

Computed tomographic imaging of individual PMMA-embedded CTBs was performed in the transverse and sagittal planes, as previously described (Figure 1). Hounsfield units were converted to PPED.[9] One transverse and sagittal slice of each bone was selected at the midpoint of the proximodistal and mediolateral planes, respectively. From these images, BMD was assessed in 2 ways. First, BMD was measured in 6 ROIs (area, 0.79 mm) located midway between the proximal and distal articular surface of the CTB in the sagittal plane (**Figure 2**). It was then measured adjacent to the dorsal slab fracture line in both the sagittal plane and the transverse plane. On the basis of the overall size of the fractured CTB, each bone had 2 or 3 ROIs (area, 0.79 mm) on either side of the dorsal slab fracture line. Drawings made on acetate overlays were made to measure BMD in similar anatomic locations in intact right CTBs. These BMD measurements were expressed as a ratio of the dorsal value to the plantar value. The ratio calculated from fractured CTBs was compared with ratios calculated from intact right CTBs.

Histologic preparation and evaluation—The PMMA-embedded, reconstructed CTBs were sectioned into 2 slices with a commercially available diamond saw system.[d] First, 1 slice approximately 150 µm in thickness was obtained in the midsagittal plane from each PMMA-embedded CTB. The CTBs were then reconstructed with the aid of cyanoacrylate,[c] and another slice approximately 150

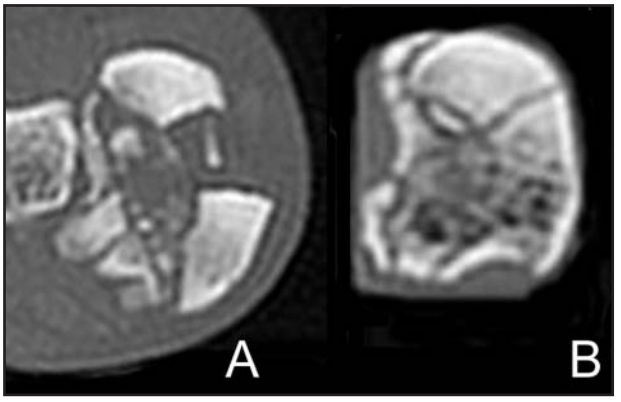

Figure 1—Computed tomographic images of a fractured right CTB from the cadaver of a racing Greyhound. A transverse section of the fractured CTB in situ (A) is compared with a transverse section of the same bone after dissection and reconstruction (B). The bone in panel B is embedded in PMMA. The medial aspect of the bone is to the right in the images.

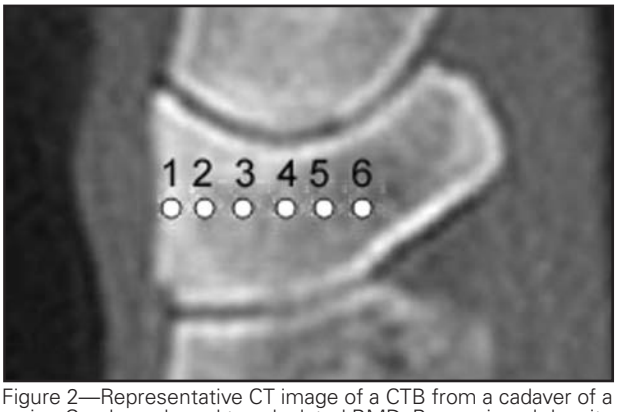

Figure 2—Representative CT image of a CTB from a cadaver of a racing Greyhound used to calculated BMD. Bone mineral density was calculated in six 1-mm ROIs on CT images in the sagittal plane of each CTB. The regions 1 through 6 were oriented in a dorsal to plantar direction.

μm in thickness was obtained in the transverse plane, located half the distance from the proximal and distal articular surfaces of the CTB. Each slice was ground to a thickness of 100 μm on a surface grinder[e] and surface stained with Masson trichrome.

Transverse and sagittal sections of each CTB were evaluated by use of light microscopy at 4X and 10X magnification. Bones were evaluated qualitatively to assess bone type and to confirm the absence of fracture repair processes. Nonscreen high-detail radiographs at a peak voltage of 32 to 35 kV and amperage of 3 mA for 90 seconds were obtained for each 100-μm section with a cabinet radiography system.[f] These radiographs were evaluated for qualitative variations in BMD.

Statistical analysis—Data analyses were performed through linear mixed-effects modeling with the aid of statistical software.[g] The models included the following factors: fracture status (fractured vs nonfractured), bone identity (right vs left), and either ROI or BMD ratio (outcome). All 2- and 3-way interactions among these factors were evaluated. Values of $P < 0.05$ were considered significant.

Results

Fracture evaluation—Six dogs had fractures in the right CTB. Findings of standard radiography, CT, and gross evaluation of CTB fractures were in agreement, and all allowed correct identification of 5 type IV (dorsal and medial slab) fractures and 1 type II (dorsal slab) fracture of the right CTB. In addition to these fractures, 5 dogs had additional tarsal bone fractures. None of the 6 dogs with fractures had evidence of fracture healing on imaging or gross evaluation. No injury was identified in the contralateral tarsus in any of these dogs. The remaining 6 dogs were confirmed free of injury in both tarsi via radiography, CT, and gross evaluation.

BMD—When the BMDs from all 6 sagittal ROIs were combined for both right and left CTBs, dogs that had a fracture had greater BMD than did dogs without a fracture ($P = 0.001$; **Figure 3**). There was no difference in summed BMD between fractured and intact right CTBs ($P = 0.55$). When each ROI was evaluated separately, however, the BMD in region 1 of fractured CTBs was greater than the BMD in region 1 in dogs that did not sustain a CTB fracture (**Figure 4**; **Table 1**). Fractured right CTBs had greater BMD in regions 2 through 4 than did contralateral CTBs from dogs with fractures or both CTBs from dogs without fractures. Among dogs that did not sustain CTB fracture, there were no significant differences in BMD between right and left CTB in any region. The BMD ratio in the regions of the dorsal slab fracture was not significantly different between fractured and intact right CTBs in both the sagittal and transverse planes.

Histologic evaluation—The cross-sectional area of right CTBs was subjectively greater than that of left CTBs, primarily because of periosteal bone formation that was present on the dorsal and medial aspects of the bones. Absolute measurement of total bone area was not possible in several fractured bones because of comminution in the plantar process and the plantarodistal aspects of the bone. Evaluation of the histologic sections revealed that the dense bone in the dorsal region of both the fractured and intact CTBs was composed of primarily lamellar, nonosteonal, compact bone. Several sections had a mild degree of osteonal remodeling present in this region. Fractured right CTBs had increased BMD attributable to coalescence and thickening of

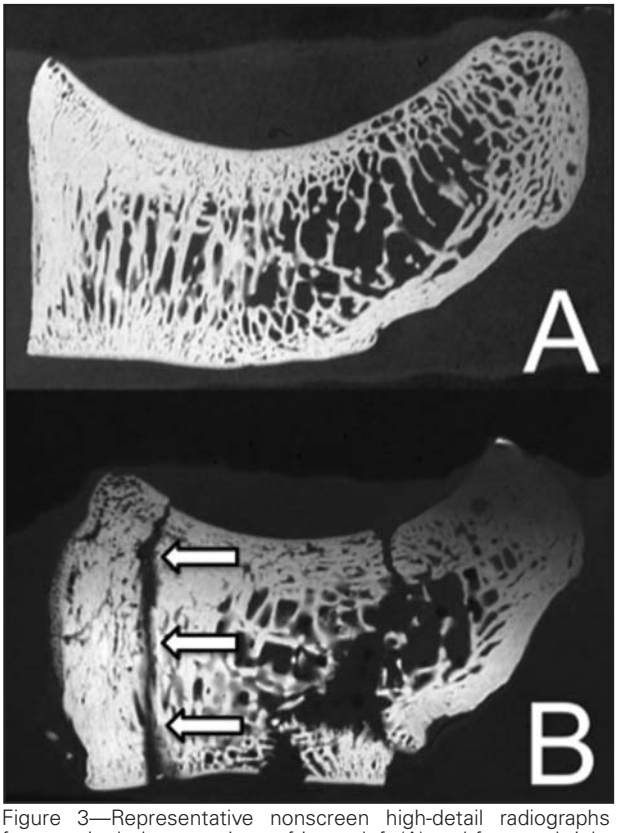

Figure 3—Representative nonscreen high-detail radiographs from sagittal plane sections of intact left (A) and fractured right (B) CTBs from the cadaver of a racing Greyhound. The proximal articular surface, the talocentral joint, is uppermost in both panels, with the dorsal aspect of the bone facing to the left. Increased BMD is evident in the fractured CTB, compared with BMD in the nonfractured CTB. The dorsal slab fracture is located in compact bone through regions of increased BMD (arrows).

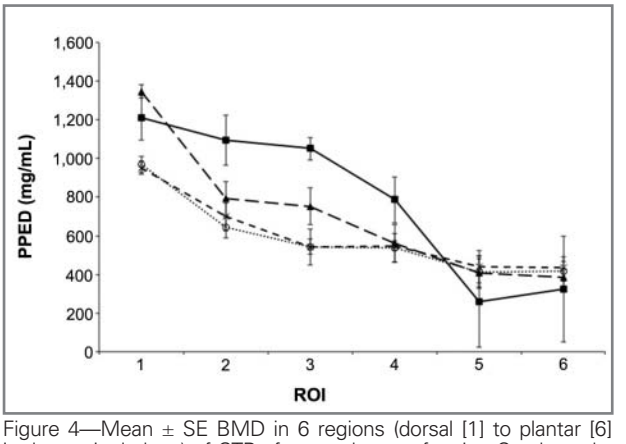

Figure 4—Mean ± SE BMD in 6 regions (dorsal [1] to plantar [6] in the sagittal plane) of CTBs from cadavers of racing Greyhounds. Dogs with fracture of the right CTB (solid line) had significantly ($P < 0.05$) greater BMD at regions 2, 3, and 4 than in the contralateral nonfractured left CTB (long-dashed line) and the right (short-dashed line) and left (dotted line) CTBs from Greyhounds without a CTB fracture.

Table 1—Bone marrow density (PPED [mg/mL]) in 6 ROIs in both CTBs from cadavers of racing Greyhounds with a fracture in the right CTB (n = 6 dogs) and Greyhounds with nonfractured CTBs (6).

		Dogs with fracture			Dogs without fracture		
ROI	CTB	25th percentile	Mean	75th percentile	25th percentile	Mean	75th percentile
1	Right	1,138.8	1,211.1	1,273.1	905.9	952.2	973.4
	Left	1,296.2	1,346.3	1,368.6	930.2	969.6	1,031.0
2	Right	925.1	1,094.2[a]	1,247.1	575.6	698.3[b]	817.3
	Left	739.1	791.2[b]	866.6	607.4	644.8[b]	661.5
3	Right	934.8	1,050.4[a]	1,136.4	347.6	543.0[b]	731.7
	Left	723.1	753.1[b]	851.6	497.5	543.3[b]	623.4
4	Right	561.7	785.8[a]	1,002.3	491.5	548.7[b]	586.5
	Left	513.7	559.7[b]	679.9	470.4	538.3[b]	528.8
5	Right	−14.0	258.9	508.9	307.5	438.4	553.0
	Left	295.3	407.4	498.8	285.6	411.2	431.5
6	Right	184.5	324.3	707.9	361.3	434.1	446.7
	Left	290.0	385.1	474.3	332.2	414.9	535.8

[a,b]Different superscript letters indicate a significant ($P < 0.05$) difference between groups and between sides within the same ROI.

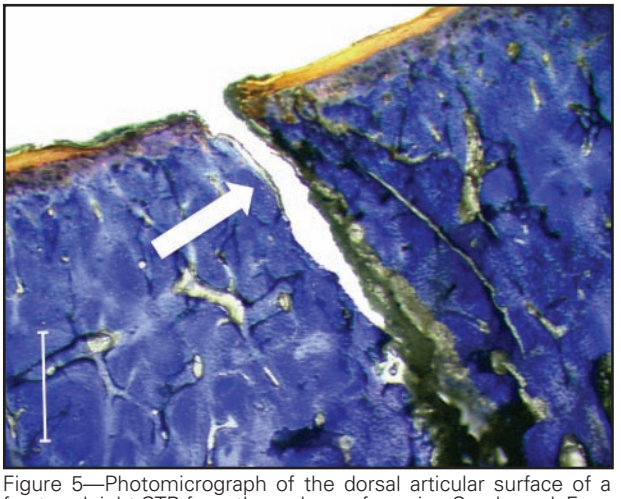

Figure 5—Photomicrograph of the dorsal articular surface of a fractured right CTB from the cadaver of a racing Greyhound. Fractures occurred through zones of increased BMD. The fracture line is indicated (arrow). Bar = 1.0 mm; Masson trichrome stain.

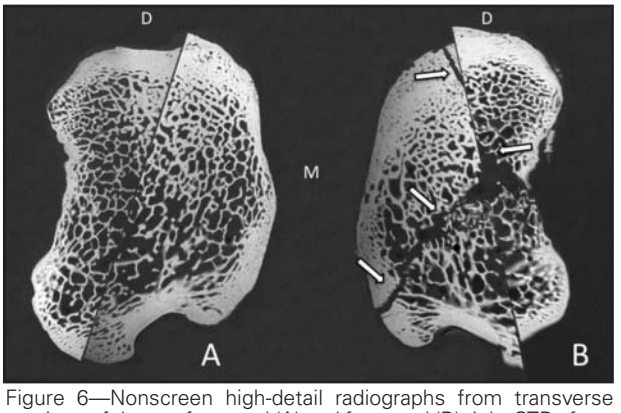

Figure 6—Nonscreen high-detail radiographs from transverse sections of the nonfractured (A) and fractured (B) right CTBs from the cadaver of a racing Greyhound. The BMD in the dorsal (D) and medial (M) aspects of the fractured CTB was greater than in the nonfractured CTB and was attributable to thickening and coalescence of trabeculi. The original fracture line is indicated (arrows).

trabeculae and a decrease in the marrow space on the dorsal and plantar aspects of the dorsal slab fracture plane. The fractures traversed through the dorsal and midbody regions of the CTB, which consisted of bone that was uniformly and grossly increased in density, compared with the density in other regions (**Figure 5**). This response was most prominent on the dorsal and medial aspects of the CTB (**Figure 6**). Periosteal modeling was evident on the dorsal slab of fractured CTBs, which primarily consisted of woven bone, but was not seen in the contralateral intact CTBs.

Discussion

Orthopedic fatigue fractures pose a considerable problem for human, equine, and canine athletes.[4,10–12] These fractures occur most commonly in long bones; data on naturally occurring stress fractures in cuboidal bones are sparse.[5,10,13–18] In diaphyseal bone, fatigue fractures have been hypothesized to occur in response to microdamage within bone.[1,7,13] Cyclic loading of long bones results in an increase in cortical size and microdamage (ie, microcracks). Fatigue fractures are believed to occur because of an imbalance between microdamage formation and repair by remodeling: microcracks accumulate until catastrophic failure occurs through crack propagation or coalescence.[1,2,7,11,19]

Less is known about stress fractures in cuboidal bones. Cuboidal bones have a characteristic anatomic structure, consisting of ≥ 2 articular surfaces, an outer shell of cortical bone, and inner trabecular bone. This structure of cuboidal bones may cause them to behave differently than diaphyseal bone. The CTB is a unique cuboidal bone. The largest of its 7 articular surfaces is the proximal concave articulation with the talus. Because of the size and shape of that articulation, the human navicular tarsal bone is suspected to be primarily subjected to compressive loading[3]; however, the load distribution patterns across canine CTBs have not been identified. The concave shape of the proximal articular surface may distribute stress and strain in unique ways, resulting in adaptive modeling and remodeling that may contribute meaningfully to stress fractures that are commonly seen in this bone.[2,3]

The counterclockwise racing pattern and asymmetric loading of the CTB in racing Greyhounds result

in preferential fracture of the right CTB. In addition to asymmetric loading during turns, Greyhounds do not slow their foot contact with the ground and, as a result, have a 71% increase in effective body weight on the limb during each step.[20] Although the magnitude and distribution of these forces on CTBs have not been evaluated in vivo, this increase in acute loading of the limb may provide the supraphysiological load needed to push the limits of bone strength, even in a well-conditioned dog.

Nonfractured CTBs of racing Greyhounds have features of asymmetric modeling and remodeling.[2] Right CTBs have evidence of cortical bone thickening, coalescence of trabeculae, and increased BMD, in comparison with left CTBs.[2] Microcracks within the bone matrix are more dense and have a greater length in intact right CTBs, than in the left counterparts.[1] Examination of the dorsal slab fragments of naturally occurring right CTB fractures of Greyhounds revealed large branching arrays of microcracks in a previous study.[19] The relationship of matrix microdamage, asymmetric modeling, and remodeling to the occurrence of CTB fracture is unclear because entire fractured right CTBs from racing Greyhounds have not been extensively evaluated. In the present study, fatigue fractures in the CTBs of racing Greyhounds were examined, revealing a significant difference in BMD in right CTBs that fractured, compared with the BMD in those that did not. Although the periosteal bone response in right CTBs was similar to observations made in another study,[2] we identified unique differences in fractured bones that have not previously been reported. Fractures occurred through a region of increased BMD in the dorsal and middorsal regions of the CTB. These new data support that site-specific remodeling of the CTB occurs and suggest that the degree of remodeling may be directly related to fracture occurrence.

Previously, only the dorsal region of right CTBs was reported to have increased BMD relative to other regions.[2] The increase in BMD within the more plantar regions of fractured CTBs in our study may suggest a progressive process of uncoupled bone remodeling resulting in bone that is too dense to sustain the applied loads. A correlation between increased BMD and fracture occurrence has been reported for humans that received chronic bisphosphonate treatment.[21,22] In such purposeful circumstances of induced uncoupled bone remodeling, it has been hypothesized that the bone, although more dense than before treatment, was also more brittle, predisposing patients to fatigue fracture.[21,22]

Cyclic loading of bones can cause reorientation and stiffening of the subchondral bone,[23] and this may contribute to CTB fracture in some dogs. Investigation into the subchondral bone and trabecular orientation in the navicular tarsal bone of human athletes would be interesting. Microhardness testing of Greyhound CTBs may yield insight into material properties of the combined mineral and organic matrix and might reveal additional information regarding etiology of fracture in this breed.

Among dogs in the present study, the BMD ratio from locations on either side of the dorsal slab fracture plane was not different between fractured and intact right CTBs. This indicates that there was not a unique density differential in the dorsal slab region in bones that sustained a fracture. Therefore, a large modulus mismatch in this region of bone may not have played a role in the occurrence of fracture. Data from the present study did not support our hypothesis that CTB fractures occur through a transition zone of bone with differing densities. Instead, the dorsal and midbody regions had similar and increased BMD, relative to other measured regions, and the fractures occurred through these regions of greater uniform density.

Additional postmortem evaluation, including micro-CT, microhardness testing, trabecular compression testing, and immunohistochemical analysis, might aid in elucidating the cause of CTB fractures in racing Greyhounds. Linear prospective studies to investigate in vivo BMD and medullary cavity changes in response to training could provide important information. Differences in BMD in the present study were detected by means of diagnostic equipment that is available in veterinary practice and may be used for future clinical studies. Nuclear scintigraphy, magnetic resonance imaging, dual energy x-ray absorptiometry, and peripheral quantitative CT may be used to evaluate lower extremity stress fracture in live subjects.[24] It is possible that with prospective screening, changes within a CTB could be detected prior to catastrophic failure.

The present study had several limitations, including the small sample size and presumably consequent limited power to detect differences. Little was known about the details of the racing histories, age, or sex of the Greyhounds used, and these factors may play a role in the magnitude and pattern of modeling and remodeling changes in CTBs.[12] Although all CTB fractures contained a dorsal slab component, each had unique fracture patterns that also introduced variability into the analysis. Additionally, the study involved one 1-mm bone slice in 2 planes for each dog, and it is possible that the changes in these slices were not representative of the bone in its entirety.

The data reported here support the existence of site-specific modeling and remodeling in fractured right CTBs of racing Greyhounds. The changes in these bones differed from those in intact CTBs and may represent a progression of changes caused by excessive matrix microdamage or brittle bone quality. Fractures occurred through the dorsal and midbody regions of the right CTB. The dorsal and midbody regions had a uniformly increased BMD, relative to other measured regions of the CTB. This finding does not support the hypothesis that CTB fractures occur by way of a modulus mismatch created by adjacent bone of substantially different BMD. Additional investigation is warranted into the material properties of the CTB to allow identification of additional factors that may play a role in the pathogenesis of CTB fracture in racing Greyhounds and other athletes.

a. Picker PQS, Philips Medical Systems NA, Bothell, Wash.
b. Dipotassium phosphate phantom, model 3T, Mindways Software Inc, San Francisco, Calif.
c. The Original Super Glue, Super Glue Corp, Rancho Cucamonga, Calif.

d. Model 340CP, Exakt Technologies Inc, Oklahoma City, Okla.
e. EXAKT Technologies, Exakt Technologies Inc, Oklahoma City, Okla.
f. Faxitron, model 43855A, Faxitron X-ray LLC, Lincolnshire, Ill.
g. SAS, version 9.1.3, SAS Institute Inc, Cary, NC.

References

1. Muir P, Johnson KA, Ruaux-Mason CP. In vivo matrix microdamage in a naturally occurring canine fatigue fracture. *Bone* 1999;25:571–576.
2. Johnson KA, Muir P, Nicoll RG, et al. Asymmetric adaptive modeling of central tarsal bones in racing Greyhounds. *Bone* 2000;27:257–263.
3. Khan KM, Brukner PD, Kearney C, et al. Tarsal navicular stress fracture in athletes. *Sports Med* 1994;17:65–76.
4. Boudrieau RJ, Dee JF, Dee LG. Central tarsal bone fractures in the racing Greyhound: a review of 114 cases. *J Am Vet Med Assoc* 1984;184:1486–1491.
5. Burr DB. Bone, exercise and stress fractures. *Exerc Sport Sci Rev* 1997;25:171–194.
6. Martin RB. Mathematical model for repair of fatigue damage and stress fracture in osteonal bone. *J Orthop Res* 1995;13:309–316.
7. Taylor D. Bone maintenance and remodeling: a control system based on fatigue damage. *J Orthop Res* 1997;15:601–606.
8. Dee JF, Dee J, Piermattei DL. Classification, management, and repair of central tarsal fractures in the racing Greyhound. *J Am Anim Hosp Assoc* 1976;12:398–405.
9. Samii VF, LesClifford M, Schulz KS, et al. Computed tomographic osteoabsorptiometry of the elbow joint in clinically normal dogs. *Am J Vet Res* 2002;63:1159–1166.
10. Bennell KL, Malcolm SA, Thomas SA, et al. The incidence and distribution of stress fractures in competitive track and field athletes. *Am J Sports Med* 1996;24:211–217.
11. Brukner P, Bradshaw C, Khan KM, et al. Stress fractures: a review of 180 cases. *Clin J Sports Med* 1996;6:85–89.
12. Nunamaker DM, Butterweck DM, Provost MT. Fatigue fractures in Thoroughbred racehorses: relationships with age, peak bone strain, and training. *J Orthop Res* 1990;8:604–611.
13. Burr DB, Milgrom C, Boyd RD, et al. Experimental stress fractures of the tibia. Biological and mechanical aetiology in rabbits. *J Bone Joint Surg Br* 1990;72:370–375.
14. Ingalls J, Wissman R. The os supranaviculare and navicular stress fractures. *Skeletal Radiol* 2011;40:937-941.
15. Lipscomb VJ, Lawes TJ, Goodship AE, et al. Asymmetric densiometric and mechanical adaptation of the left fifth metacarpal bone in racing Greyhounds. *Vet Rec* 2001;148:308–311.
16. Bennell KL, Malcolm SA, Wark JD, et al. Models for the pathogenesis of stress fractures in athletes. *Br J Sports Med* 1996;30:200–204.
17. McBryde AM Jr. Stress fractures in athletes. *J Sports Med* 1975;3:212–217.
18. Devas MB. Compression stress fractures in man and the Greyhound. *J Bone Joint Surg Br* 1961;43:540–551.
19. Tomlin JL, Lawes TJ, Blunn GW, et al. Fractographic examination of racing Greyhound central (navicular) tarsal bone failure surfaces using scanning electron microscopy. *Calcif Tissue Int* 2000;67:260–266.
20. Usherwood JR, Wilson AM. Biomechanics: no force limit on Greyhound sprint speed. *Nature* 2005;438:753–754.
21. Neviaser AS, Lane JM, Lenart BA, et al. Low-energy femoral shaft fractures associated with alendronate use. *J Orthop Trauma* 2008;22:346–350.
22. Capeci CM, Tejwani NC. Bilateral low-energy simultaneous or sequential femoral fractures in patients on long-term alendronate therapy. *J Bone Joint Surg Am* 2009;91:2556–2561.
23. Radin EL, Orr RB, Kelman JL, et al. Effect of prolonged walking on concrete on the knees of sheep. *J Biomech* 1982;15:487–492.
24. Moran DS, Evans RK, Hadad E. Imaging of lower extremity stress fracture injuries. *Sports Med* 2008;38:345–356.